Electronic Supplementary Material (ESI) for Journal of Materials Chemistry A.

Supplementary Information

P vacancies enriched 3D hierarchical reduced cobalt phosphide as a precursor template of defects engineering for efficient water oxidation

Xichen Zhou,[a] Hong Gao,[a] Yifan Wang,[a] Zhen Liu,[a] Junqi Lin,[a] and Yong Ding*[ab]

[a]*State Key Laboratory of Applied Organic Chemistry, Key Laboratory of Nonferrous Metal Chemistry and Resources Utilization of Gansu Province and College of Chemistry and Chemical Engineering, Lanzhou University, Lanzhou 730000, China.*

[b]*State Key Laboratory for Oxo Synthesis and Selective Oxidation, Lanzhou Institute of Chemical Physics, Chinese Academy of Sciences, Lanzhou 730000, China.*

***Corresponding Authors:** dingyong1@lzu.edu.cn

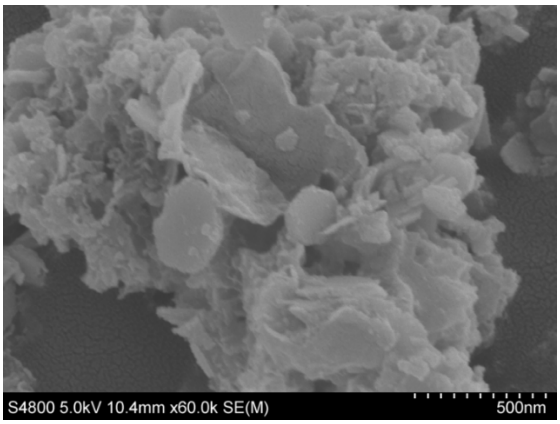

Fig. S1 The SEM image of R-CoP_x/rGO(O).

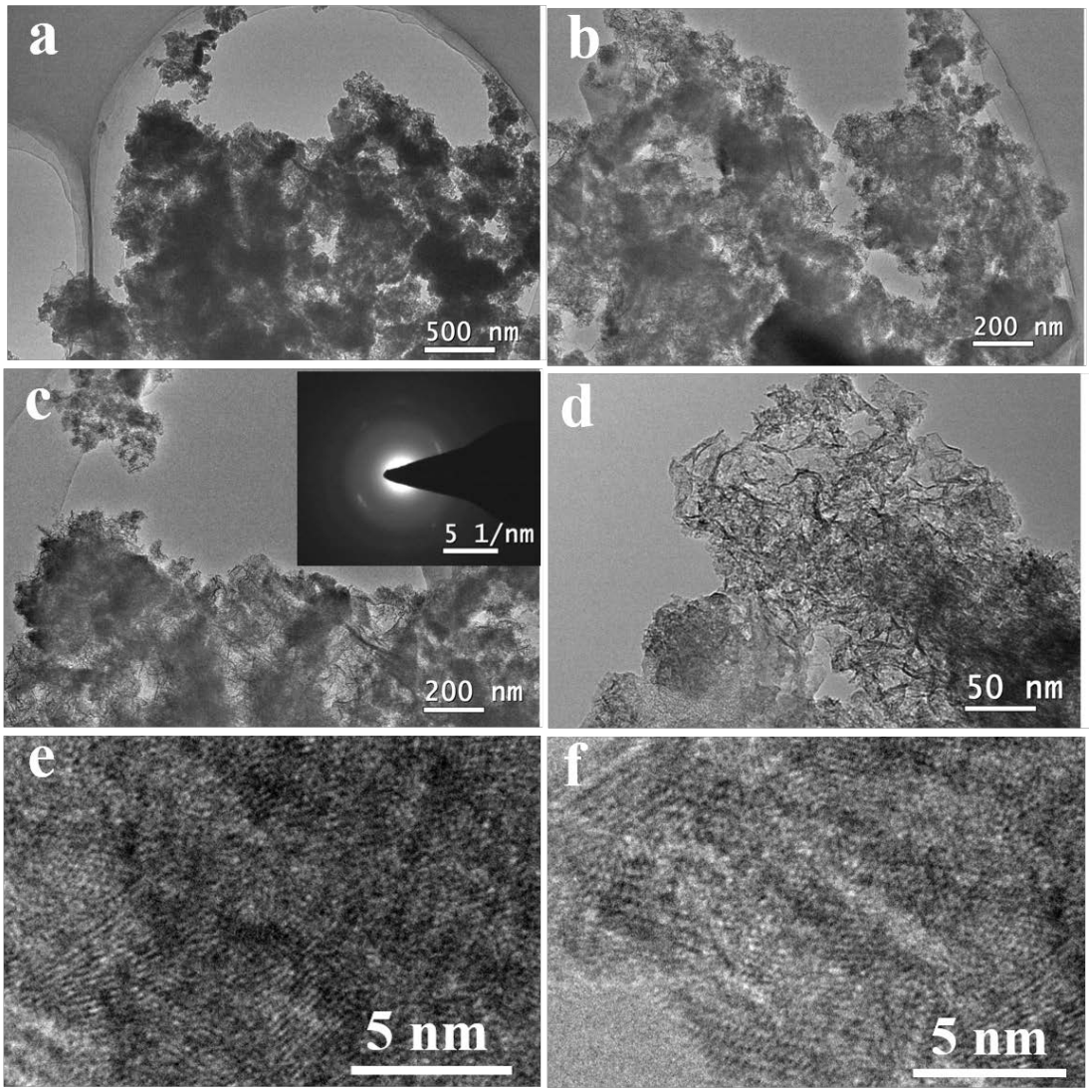

Fig. S2 The TEM, HRTEM and SAED images of R-CoP_x/rGO(O).

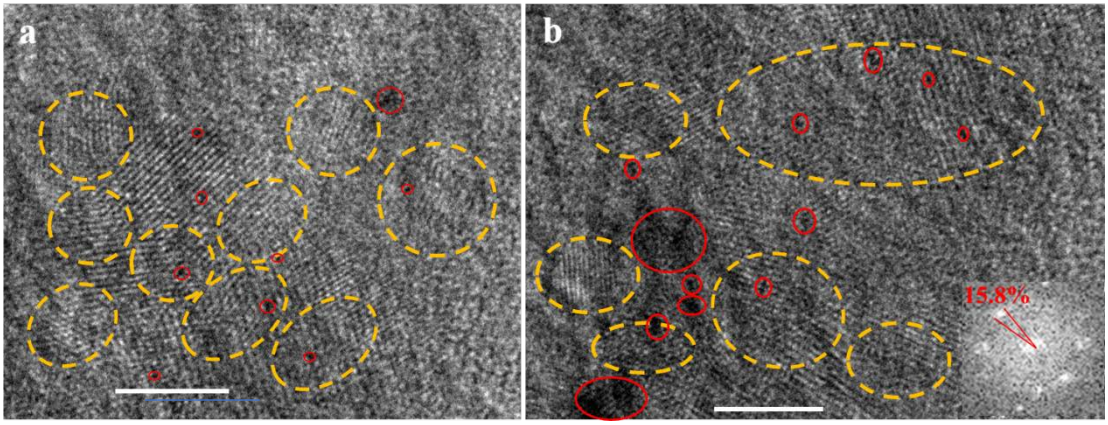

Fig. S3 (a) and (b) HRTEM images of R-CoP_x/rGO(O). Some lattice distortion regions of surface CoOOH are circled by closed yellow dash lines. Some defects of surface CoOOH are circled by closed red lines. The inset in (b) is the corresponding fast Fourier transform (FFT) image. The white scale bar represents the length of 5 nm.

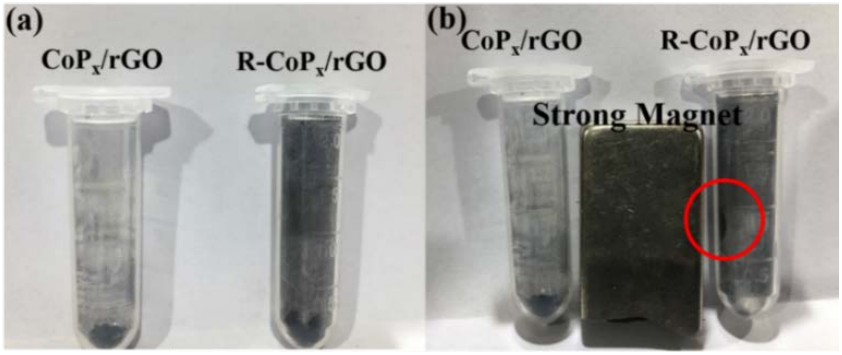

Fig. S4 (a) The photo images of CoP_x/rGO and R-CoP_x/rGO. (b) The photo images of CoP_x/rGO and R-CoP_x/rGO in the magnetic field.

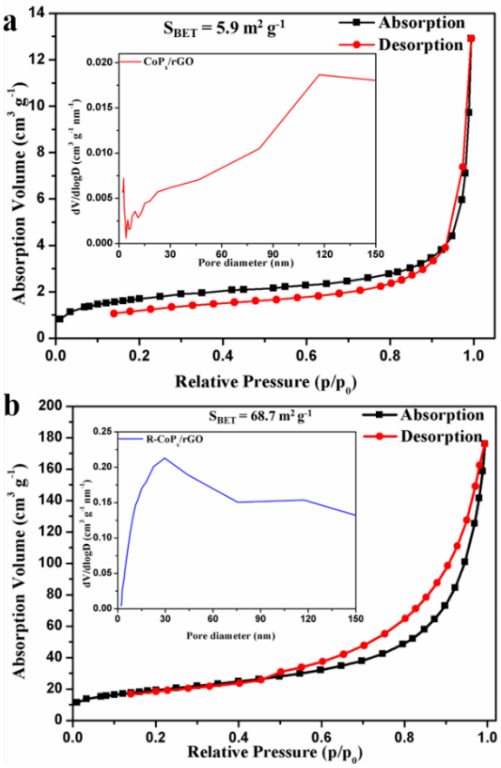

Fig. S5 N_2 adsorption/desorption isotherm curves for (a) CoP_x/rGO, and (b) R-CoP_x/rGO. Insets, the pore-size distributions of materials.

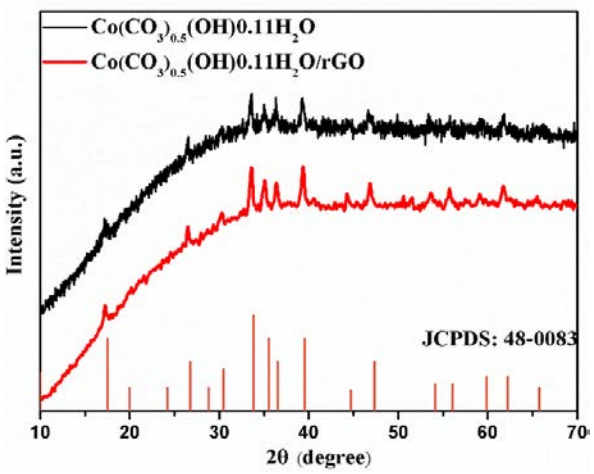

Fig. S6 PXRD patterns of $Co(CO_3)_{0.5}(OH)0.11H_2O$ and $Co(CO_3)_{0.5}(OH)0.11H_2O$/rGO. The vertical lines are the standard diffraction peaks of $Co(CO_3)_{0.5}(OH)0.11H_2O$ (JCPDS: 480083).

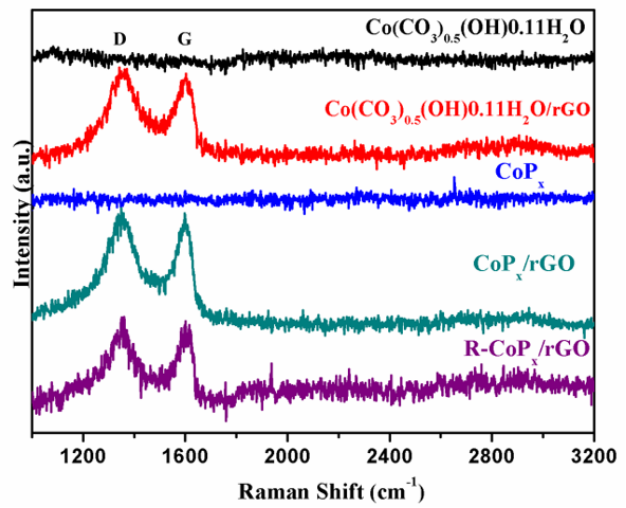

Fig. S7 Raman spectra of $Co(CO_3)_{0.5}(OH)0.11H_2O$, $Co(CO_3)_{0.5}(OH)0.11H_2O$/rGO, CoP_x, CoP_x/rGO and R-CoP_x/rGO samples.

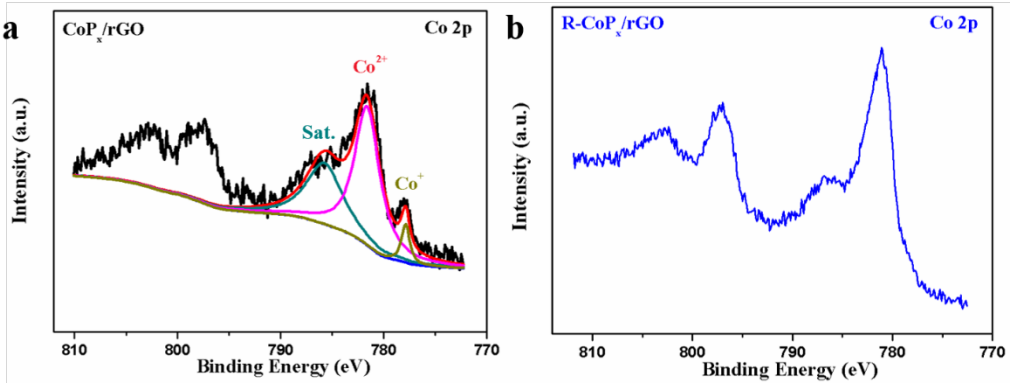

Fig. S8 The XPS Co 2p spectra of (a) CoP_x/rGO and (b) R-CoP_x/rGO.

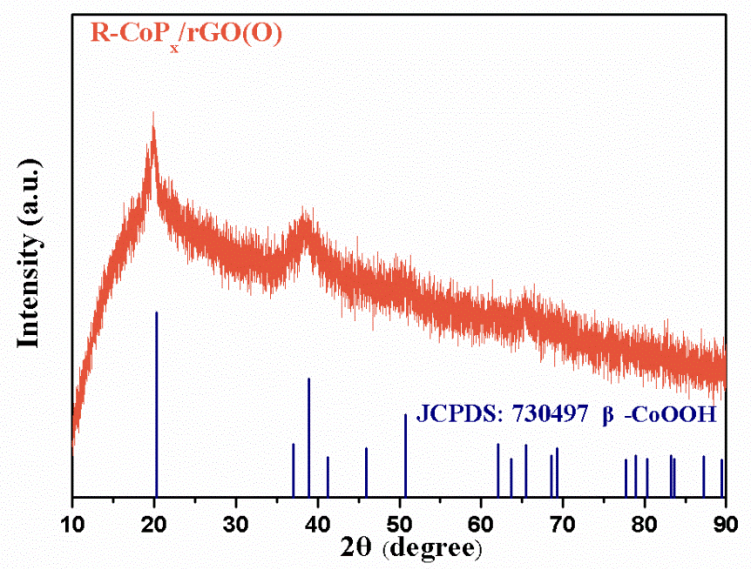

Fig. S9 XRD pattern of R-CoP$_x$/rGO(O).

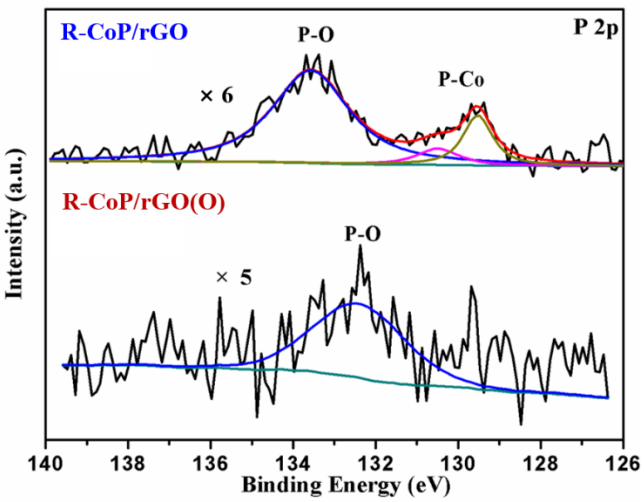

Fig. S10 XPS P2p spectra of R-CoP$_x$/rGO and R-CoP$_x$/rGO(O).

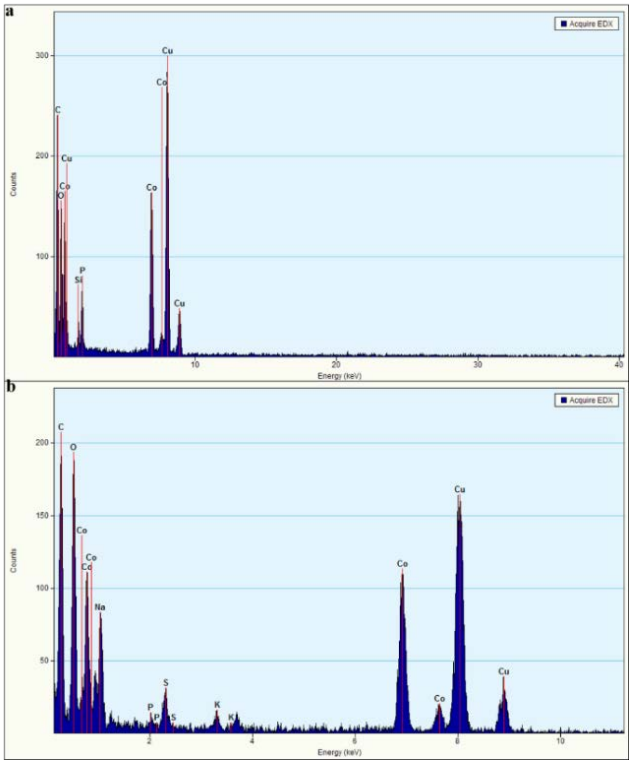

Fig. S11 (a) EDX (Energy Dispersive X-ray) measurements of R-CoP_x/rGO. (b) EDX measurements of R-CoP_x/rGO(O).

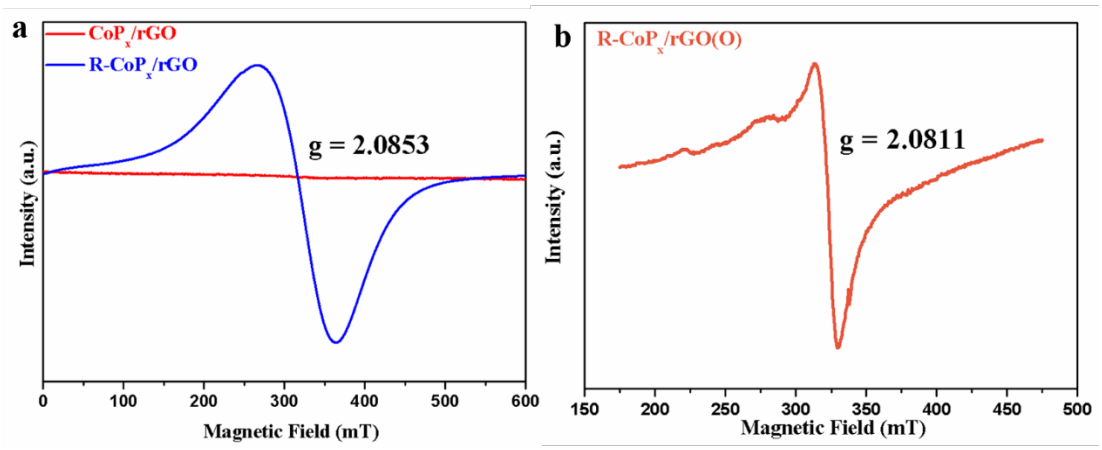

Fig. S12 Electron Paramagnetic Resonance (EPR) curves of CoP_x/rGO, R-CoP_x/rGO and R-CoP_x/rGO(O).

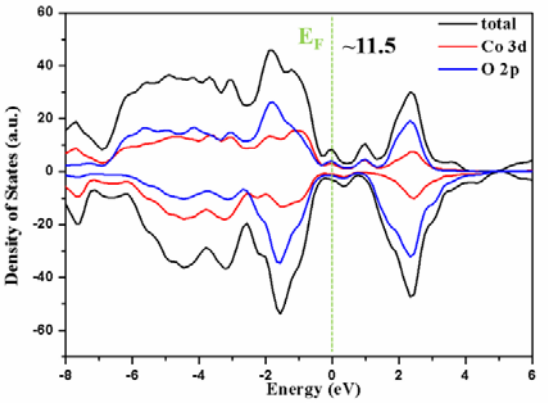

Fig. S13 DFT results. The thin shell of (101) facet exposed *β*-CoOOH.

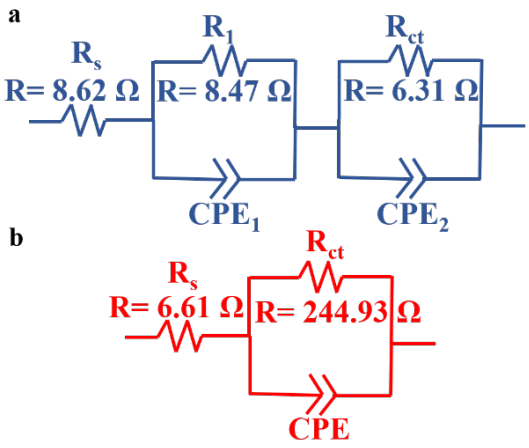

Fig. S14 Equivalent circuit diagrams of (a) R-CoP_x/rGO(O) and (b) CoP_x/rGO(O), respectively.

For R-CoP_x/rGO(O), as two independent semicircles are obtained in the Nyquist plot, two parallel components (including a polarization resistance (R_1 at high frequencies and R_{ct} at low frequencies) and a constant phase element (CPE)) are fitted in series with a resistance (R_s) from the solution and all ohmic contact. The first semicircle at high frequencies is related to the property of the electrode's surface; whereas another at low frequencies is attributed to the kinetics of the OER process. Only one semicircle is observed in the Nyquist plot of CoP_x/rGO(O), so only one component (including a polarization resistance (R_{ct}) and a constant phase element (CPE) are fitted in series with a resistance (R_s) from the solution and all ohmic contact.

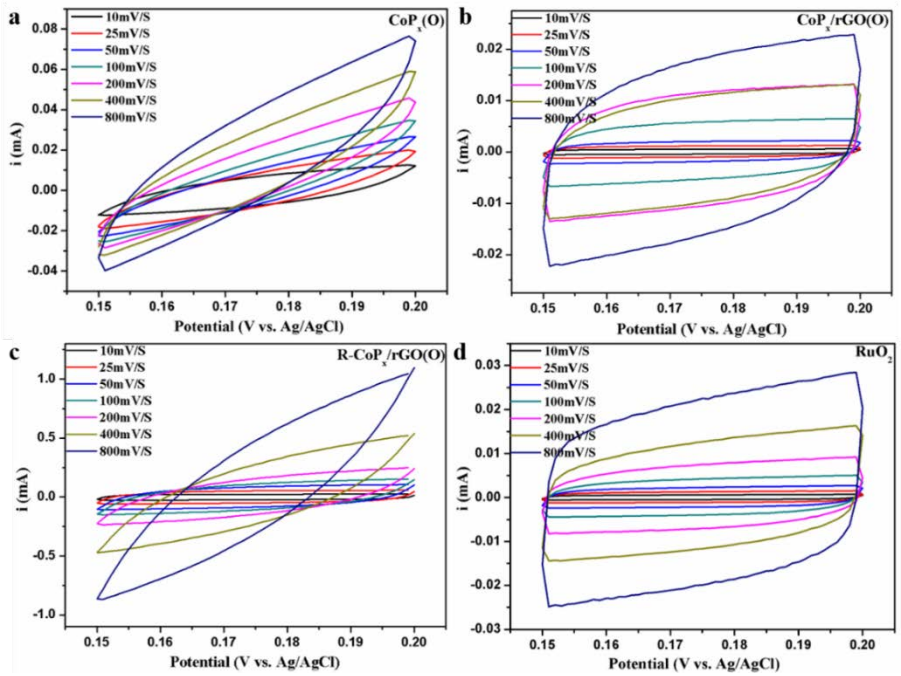

Fig. S15 CVs of CoP_x(O) (a), CoP_x/rGO(O) (b), R-CoP_x/rGO(O) (c) and RuO_2 (d) samples from 0.15 to 0.20 V vs. Ag/AgCl at various scan rates from 10 mV/s to 800 mV/s in 1.0 M KOH solution.

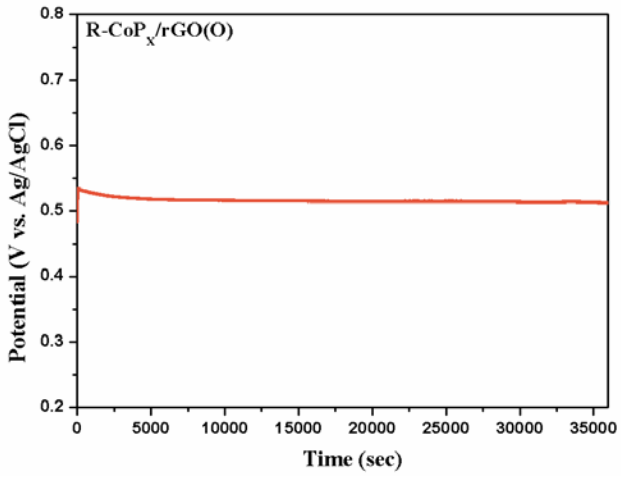

Fig. S16. Bulk electrolysis obtained by using R-CoP_x/rGO(O) as the catalyst for water oxidation in 1.0 M KOH under a fix current density of 10 mA cm^{-2}.

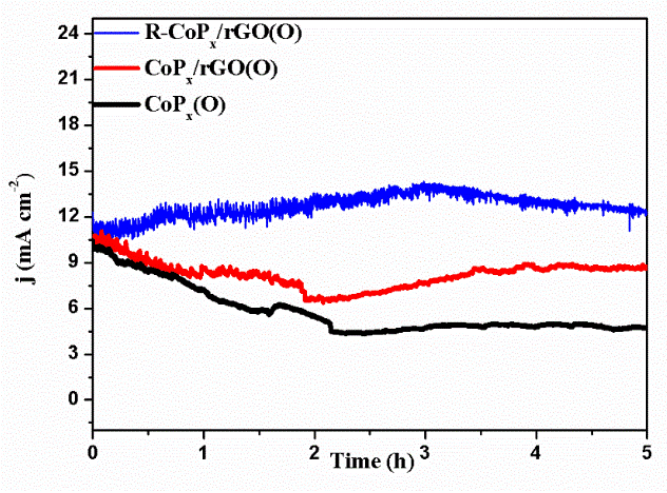

Fig. S17 Bulk electrolysis obtained by using R-CoP_x/rGO(O), CoP_x/rGO(O) and CoP_x(O) as the catalyst for water oxidation in 1.0 M KOH under overpotentials of 268 mV, 389 mV and 373 mV, respectively.

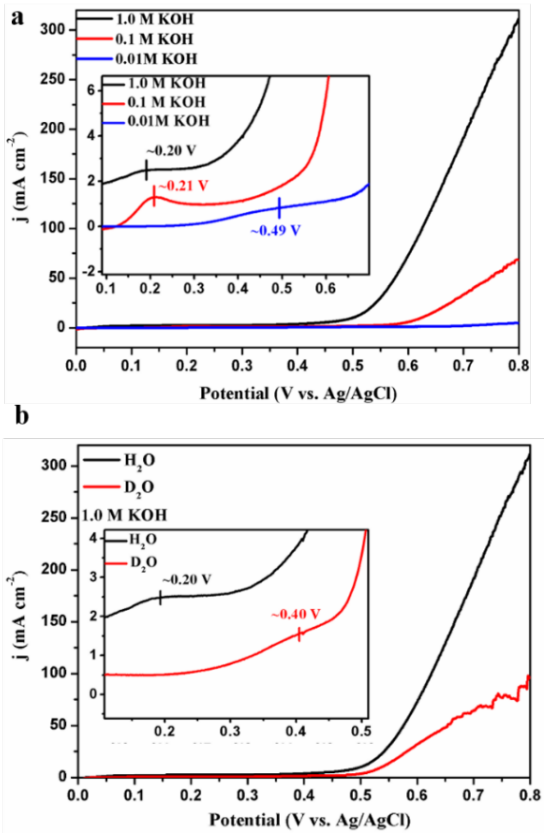

Fig. S18 (a) Linear sweep voltammograms (LSV) of R-CoP_x/rGO(O) in 1.0 M, 0.1 M and 0.01 M KOH solutions. (b) Linear sweep voltammograms (LSV) of R-CoP_x/rGO(O) in 1.0 M H_2O and D_2O solutions. The insets of (a) and (b) shows the corresponding magnifying LSV curves and the corresponding $Co^{2+/3+}$ anodic peaks.

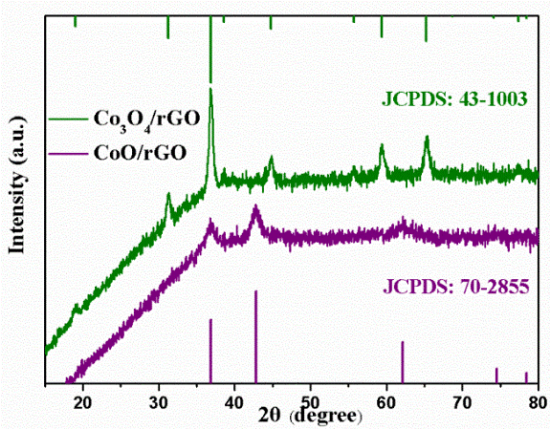

Fig. S19 PXRD patterns of Co_3O_4/rGO and CoO/rGO. The vertical lines are the standard diffraction peaks of Co_3O_4/rGO (JCPDS: 431003) and CoO/rGO (JCPDS: 702855).

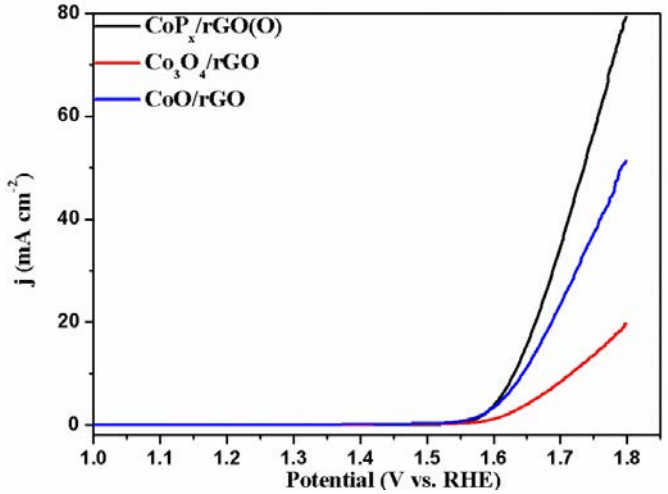

Fig. S20 Linear sweep voltammograms (LSV) of CoPx/rGO(O), Co_3O_4/rGO and CoO/rGO samples.

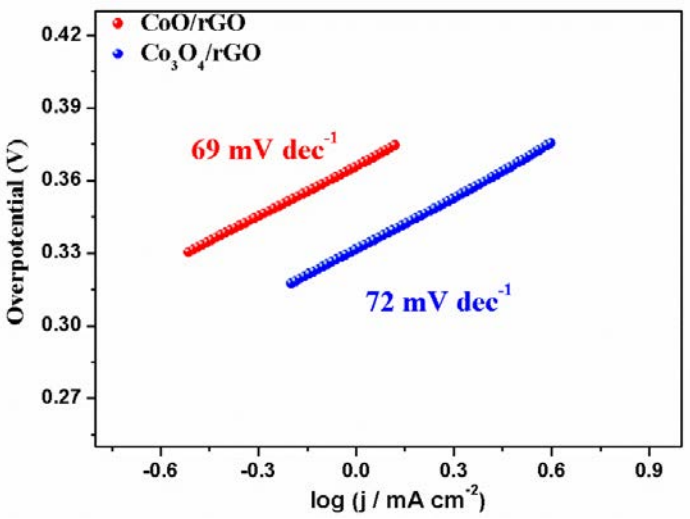

Fig. S21 Tafel slopes of Co_3O_4/rGO and CoO/rGO samples.

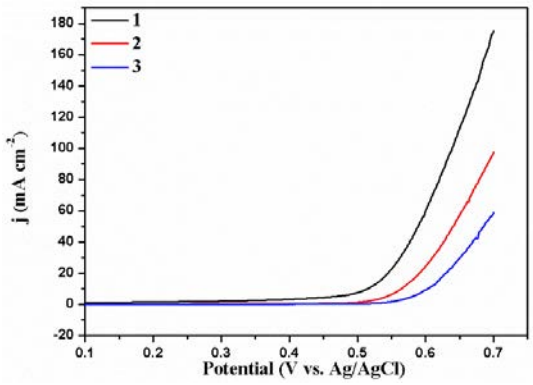

Fig. S22 The LSV curves of 1 R-CoP_x/rGO(O), 2 R-CoP_x/rGO-H_2O_2 and 3 R-CoP_x/rGO(O)-H_2O_2.

We conducted electrocatalytic experiments to confirm the formation and the effect of defects in the catalysts.

The catalyst R-CoP_x/rGO(O) is represented as 1. The obtained R-CoP_x/rGO powder was dispersed in 30% H_2O_2 solution and stirring for 20 min to fill in the defects of R-CoP_x/rGO through oxidation[1], and then the powder was collected by centrifugation, washed with deionized water for several times and dried in a vacuum oven. Finally, the sample 2 (R-CoP_x/rGO-H_2O_2) was obtained. The sample 3 was obtained as the following method. Catalyst R-CoP_x/rGO ink was dropwise added on a glassy carbon electrode and fixed by Nafion (0.5%), then dried in air. And then the R-CoP_x/rGO(O) coated glassy carbon electrode was obtained after electrochemical OER process. Afterwards, this glassy carbon electrode

with R-CoP_x/rGO(O) was immersed in 30% H_2O_2 for 20 min to fill in the defects of R-CoP_x/rGO through oxidation, and the obtained electrode is sample 3.

All electrochemical experiments were conducted using CHI760D Instrument Potentiostat at room temperature (~25℃). The typical three-electrode cell system was employed, including Ag/AgCl electrode as the reference electrode, Pt wire as the counter electrode, and glassy carbon electrode as the working electrode. The water oxidation performance of 1 is superior to 2 and 3 obviously. The relatively poorer oxygen evolution activity of 2 and 3 probably is caused by the defects in sample 2 and 3 which have been filled with oxygen. In sum, the results reveal that the formation phosphorus vacancies in the main catalysts.[1]

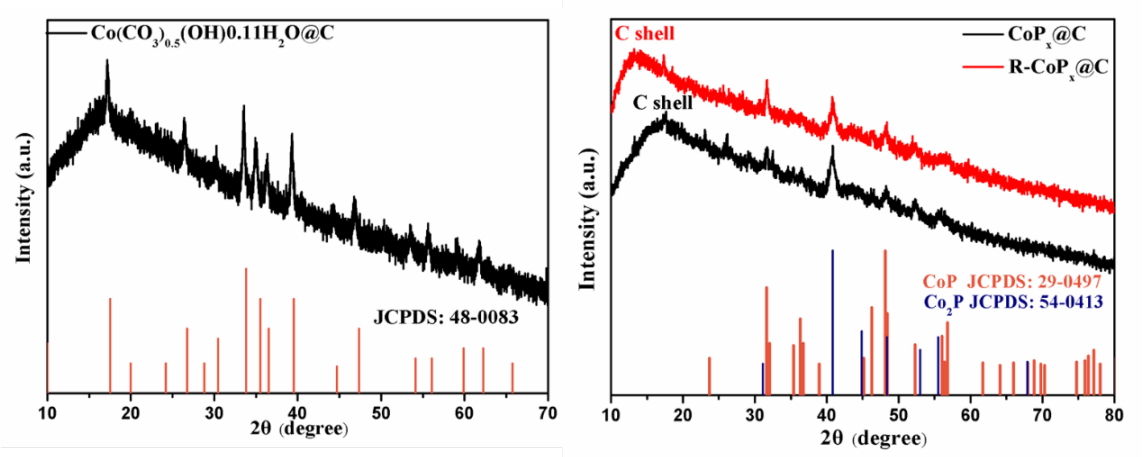

Fig. S23 (a) PXRD patterns of $Co(CO_3)_{0.5}(OH)0.11H_2O$@C. The vertical lines are the standard diffraction peaks of $Co(CO_3)_{0.5}(OH)0.11H_2O$ (JCPDS: 480083). (b) PXRD patterns of CoP_x@C and R-CoP_x@C. The vertical lines are the standard diffraction peaks of CoP (JCPDS: 290497) and Co_2P (JCPDS: 540413).

When the defects in R-CoP_x/rGO and R-CoP_x/rGO(O) are filled with oxygen, the OER performances of the R-CoP_x/rGO and R-CoP_x/rGO(O) are significantly reduced (Fig. S22), revealing the positive effect of the defects on the improvement of the catalysts' water oxidation properties.

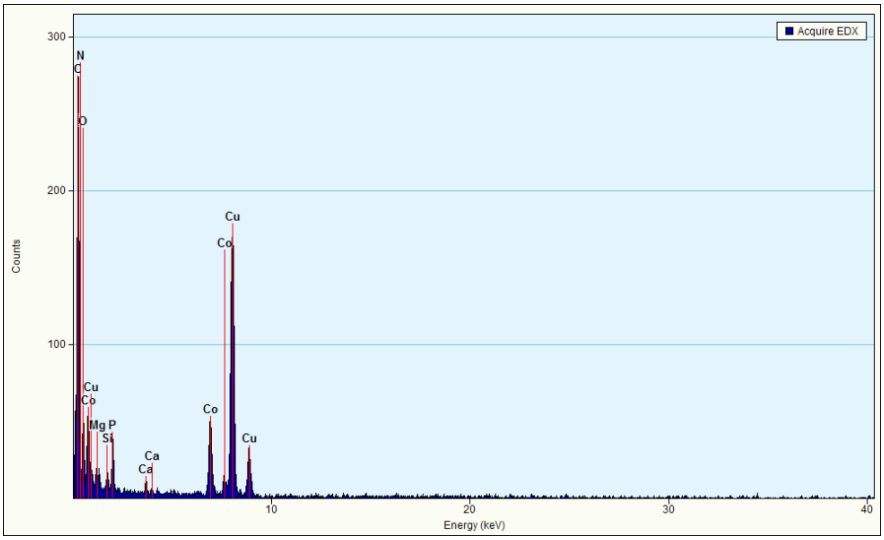

Fig. S24 Energy Dispersive X-ray measurements of R-CoP_x@C.

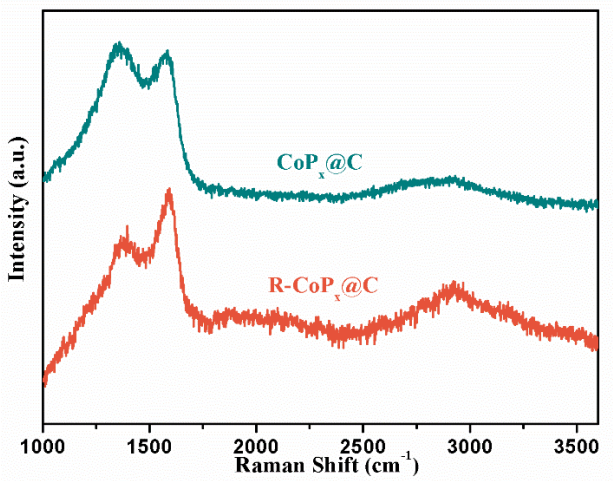

Fig. S25 Raman spectroscopy spectra of CoP_x@C and R-CoP_x@C.

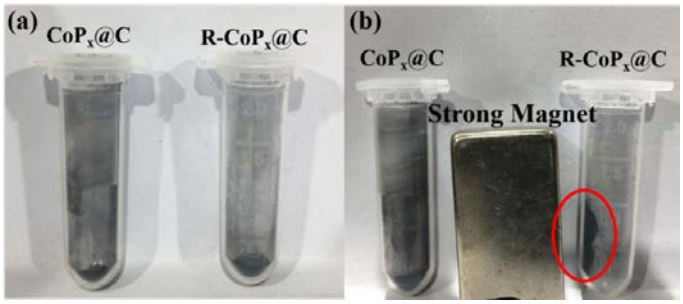

Fig. S26 (a) The photo images of CoP_x@C and R-CoP_x@C. (b) The photo images of CoP_x@C and R-CoP_x@C in the magnetic field.

Table S1. Summary of the electrochemical water oxidation activities of Co-based metal phosphides.

Catalyst	Electrolyte	η at 10mAcm^{-2} (mv)	Ref.
R-CoP_x/rGO(O)	1M KOH	268	This work
CoP_x/rGO(O)	1M KOH	389	This work
CoP_x(O)	1M KOH	373	This work
RuO_2	1M KOH	287	This work
CoP_3NAs/CFP	1M KOH	334	2
Co/CoP-5	1M KOH	340	3
CoP-based nano Needle	1M KOH	281	4
CoP_2/RGO	1M KOH	300	5
CoP hollow polyhedron	1M KOH	400	6
CoMnP	1M KOH	330	7

Reference

1. Z. Beibei, W. Lei, Z. Yajun, D. Yong and B. Yingpu, *Angew. Chem. Int. Ed.*, 2018, 57, 2248-2252.
2. T. Wu, M. Pi, D. Zhang and S. Chen, *J. Mater. Chem. A*, 2016, 4, 14539-14544.
3. Z.-H. Xue, H. Su, Q.-Y. Yu, B. Zhang, H.-H. Wang, X.-H. Li and J.-S. Chen, *Adv. Energy Mater.*, 2017, 7, 1602355-n/a.
4. P. Wang, F. Song, R. Amal, Y. H. Ng and X. Hu, *ChemSusChem*, 2016, 9, 472-477.
5. J. Wang, W. Yang and J. Liu, *J. Mater. Chem. A*, 2016, 4, 4686-4690.
6. M. Liu and J. Li, *ACS Appl. Mater. Interfaces*, 2016, 8, 2158-2165.
7. D. Li, H. Baydoun, C. N. Verani and S. L. Brock, *J. Am. Chem. Soc.*, 2016, 138, 4006-4009.